Supplementary Information for

Ice Nucleation by DNA Origami

Sarah A. Alsalhi[1,2], Jonathan Bath[3], Andrew Turberfield[3] and Walther Schwarzacher[2,4]

[1]Department of Physics, College of Science, Princess Nourah bint Abdulrahman University, Riyadh 11671, Saudi Arabia
[2]H. H. Wills Physics Laboratory, University of Bristol, Bristol BS8 1TL, U.K.
[3]Clarendon Laboratory, University of Oxford, Oxford OX1 3PU, U.K.
[4]Syed Babar Ali School of Science and Engineering, LUMS, Lahore 54792, Pakistan.

Methods

Droplet freezing experiments.

The substrates used were silcon slides with a hydrophobic coating prepared by immersion in Dimethyloctadecyl[3-(trimethoxysilyl)propyl]ammonium chloride (DMOAP) at a concentration of 0.1 to 1 % (v/v), followed by curing for an hour in an oven at 120 ^{o}C. The contact angle of water droplets on the DMOAP-coated slides was $\approx$ 90°.

To carry out an isothermal freezing experiment, an electronic microlitre pipette was used to pipette 20 droplets of volume 1 μL onto a coated slide. This was placed on a 22mm diameter pure silver heating block in the sealed sample chamber of a commercial liquid-nitrogen cooled cold stage with optical access (Linkam THMS600). The droplets were then cooled at a rate of 50 ^{o}C /min from ambient temperature to the programmed target temperature, as recorded by the platinum sensor embedded in the heating block. The target temperature was maintained for 2-3 seconds before data recording started. An OLYMPUS SZX10 Stereomicroscope with a magnification range of 0.63x - 6.3x and an affixed digital camera (Moticam 5MP) with customized illumination were used to observe droplet freezing events (figure S1). ImageJ software and the Pytorch-YOLOv5 (Python object detection algorithm) [1] were used to detect and count the unfrozen droplets. The algorithm was trained on hundreds of images of droplets to distinguish unfrozen ones, including droplets in image corners.

Temperature ramp experiments were carried out using the same apparatus. To save time, samples were cooled to a pre-selected initial temperature at 20 ^{o}C /min. Subsequently, images of the droplet array were captured as the temperature was decreased at a rate of 1 ^{o}C /min. From these images, the frozen fraction was determined as a function of the temperature.

DNA origami

1.8 mL of single-stranded template derived from the plasmid pKD1 (2646 nt, 100 nM) and short oligonucleotide staple strands (8 - 40 nt; 200 nM) was prepared in a buffer containing 12.5 mM $MgCl_2$, 10 mM Tris-HCl, 1 mM EDTA, pH 8.0. Staple and template sequences are given in [2]. Staple 9[48]-8[48] was labelled at the 5' end with Cy5, staple 11[48]-10[48] was labelled at the 5' end with Cy3. The mixture was split into two aliquots of 0.9 mL: one aliquot was heated to 85°C then cooled to 25°C at 1°C/minute to produce well folded DNA origami tiles. The other aliquot was left without further treatment to produce unfolded/mis-folded DNA tiles. Samples were analyzed using gel electrophoresis (0.7% agarose w/v in TAE buffer) and Cy3 fluorescence to visualise. A size standard (1 kb ladder, New England Biolabs) was mixed with Sybr Gold (Invitrogen) at a final concentration of 1x and run alongside the origami samples. Well folded origami tiles were diluted to 5 nM in a buffer containing 4 mM $NiCl_2$ and deposited on freshly cleaved mica for imaging using a CypherES AFM and AC40TS cantilevers.

Typical droplet images recorded during an isothermal freezing experiment

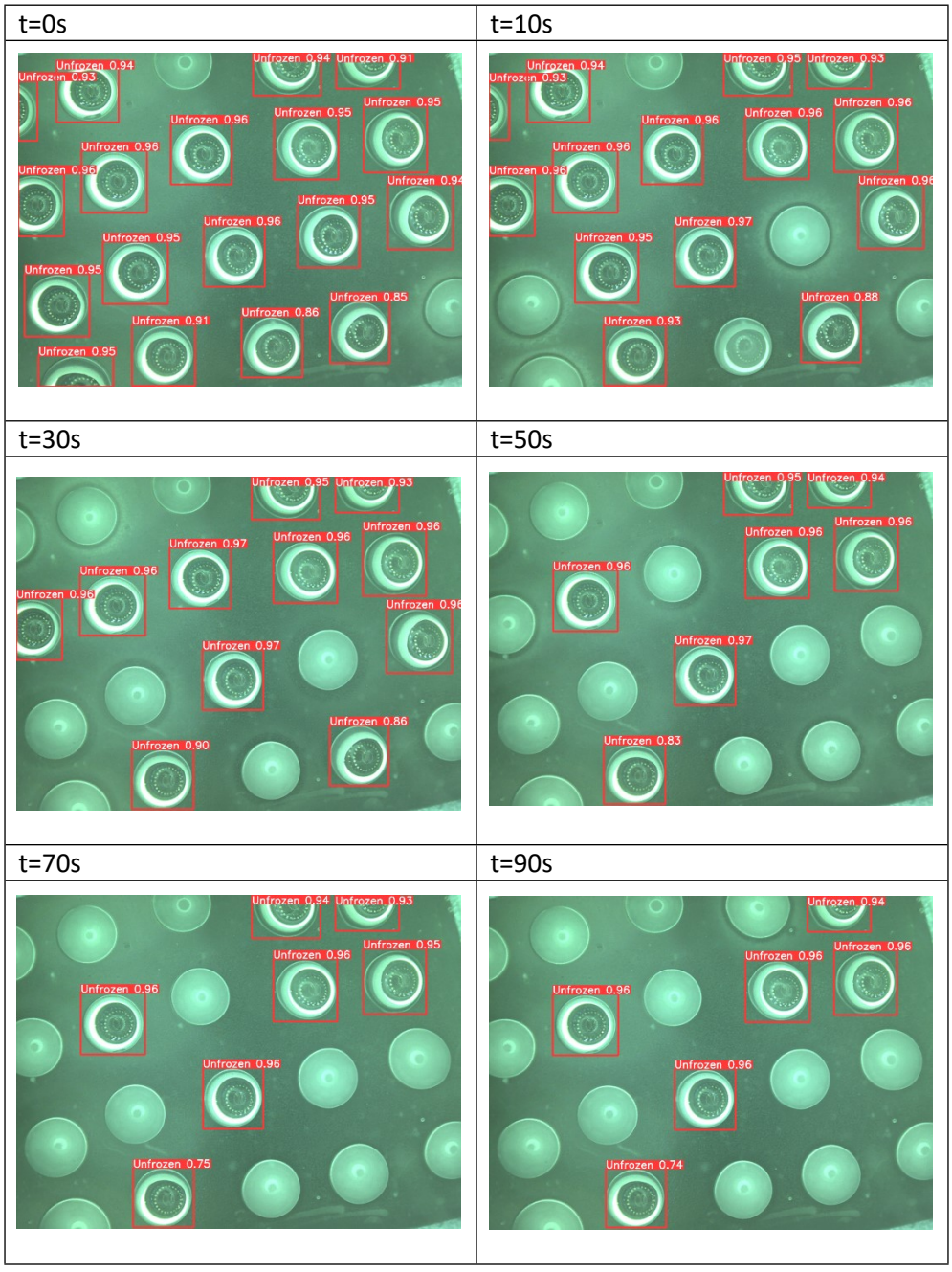

Figure S1: Droplet images recording during an isothermal freezing experiment carried out using 1 µL droplets of Tris buffer at -26°C. Unfrozen droplets are detected automatically using ImageJ software and the Pytorch-YOLOv5 Python object detection algorithm. The rings visible in the unfrozen droplets are a reflection of the lighting system.

Isothermal freezing data for annealed and unannealed DNA samples at additional temperatures

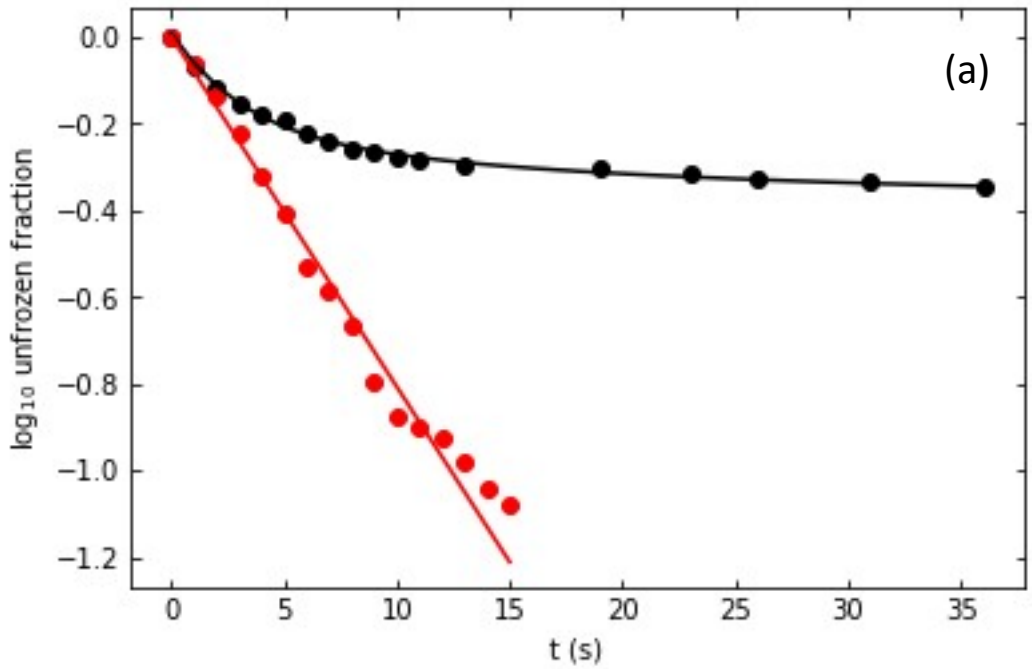

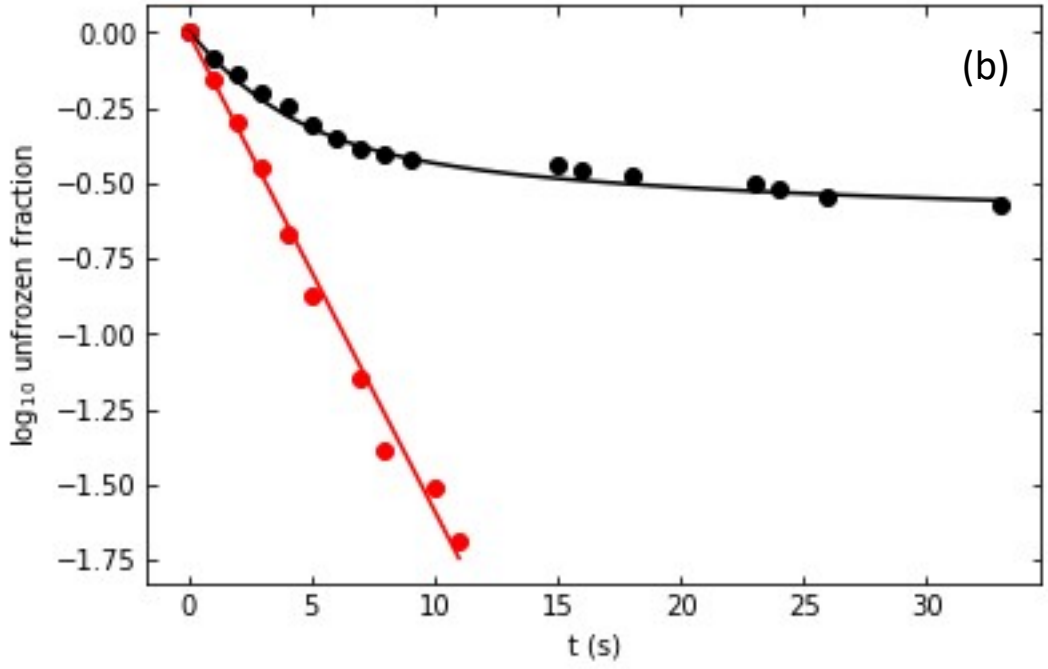

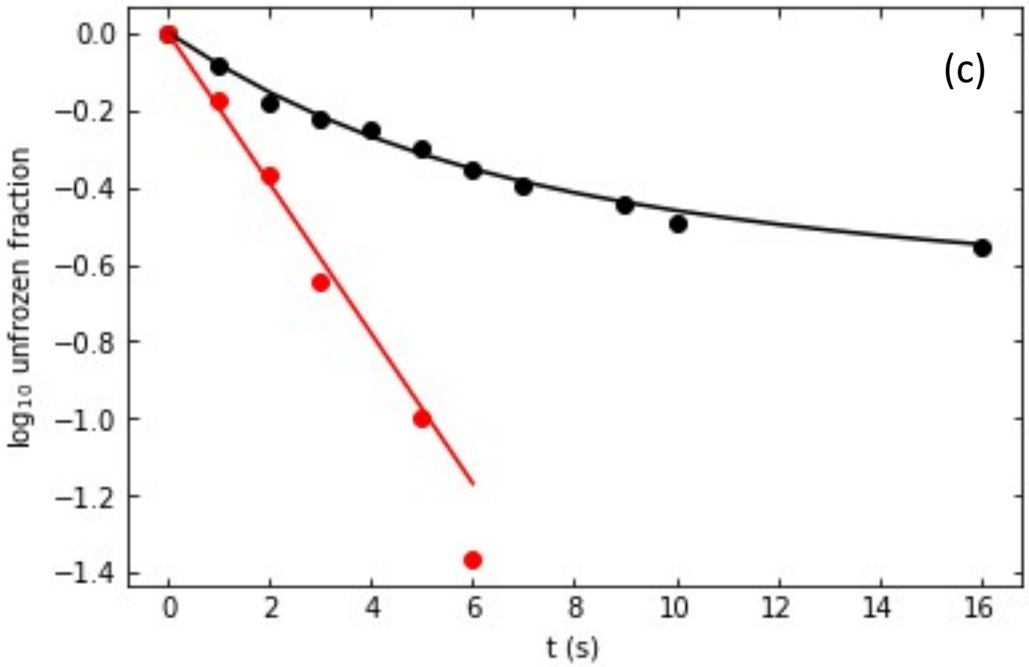
(c)
log₁₀ unfrozen fraction
0.0
−0.2
−0.4
−0.6
−0.8
−1.0
−1.2
−1.4
0
2
4
6
8
10
12
14
16
t (s)

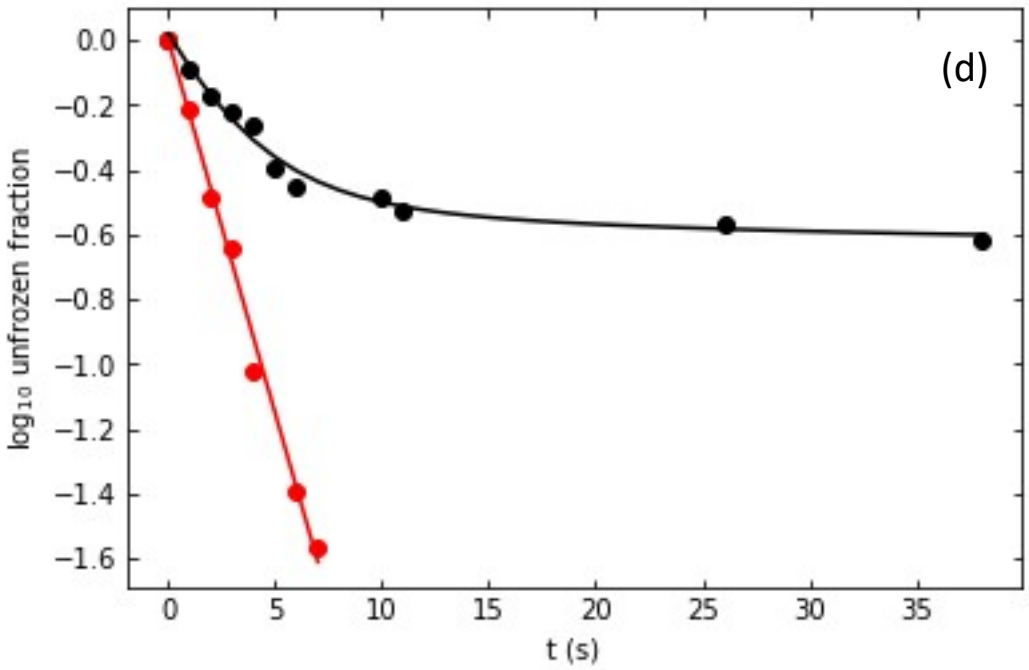
(d)
log₁₀ unfrozen fraction
0.0
−0.2
−0.4
−0.6
−0.8
−1.0
−1.2
−1.4
−1.6
0
5
10
15
20
25
30
35
t (s)

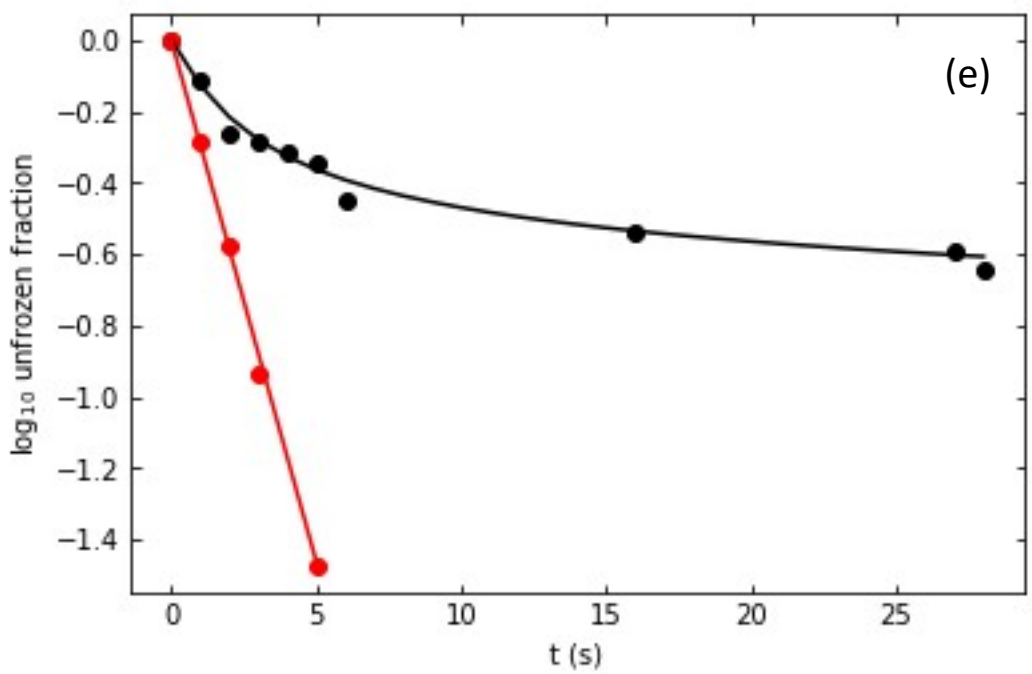

Figure S2: Isothermal freezing data for 1 μL droplets of Tris buffer containing 100 nM annealed (well-folded) DNA origami tiles (red dots) and the same concentration of unannealed origami components (black dots) at (a) -24°C; (b) -25°C; (c) -25.5°C; (d) -26°C; (e) -26.5°C. The linear fits to the annealed origami data are those that were used to plot figure 3 in the main paper. The fits to the unannealed data correspond to the values of J_0, μ_η and σ_η given in table S1. The number of droplets contributing to each set of data is given in tables S2 and S3.

Isothermal freezing data modelled using the same parameters as figure 4.

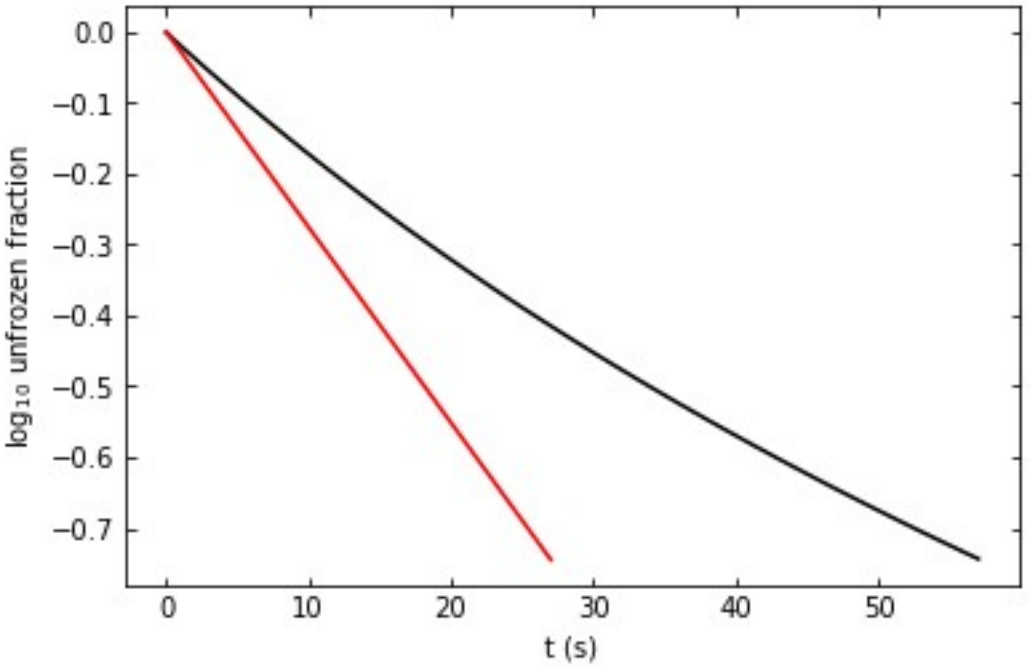

Figure S3. Modelled isothermal freezing data at -24.5 °C. The model for the annealed origami samples (red line) corresponds to $J_0 = 275$ and $\eta = 1.25 \times 10^6$. The model for the unannealed origami samples (black line) corresponds to $J_0 = 0.55$, $\mu_\eta = 12.9$ and $\sigma_\eta = 0.25$ (see main text).

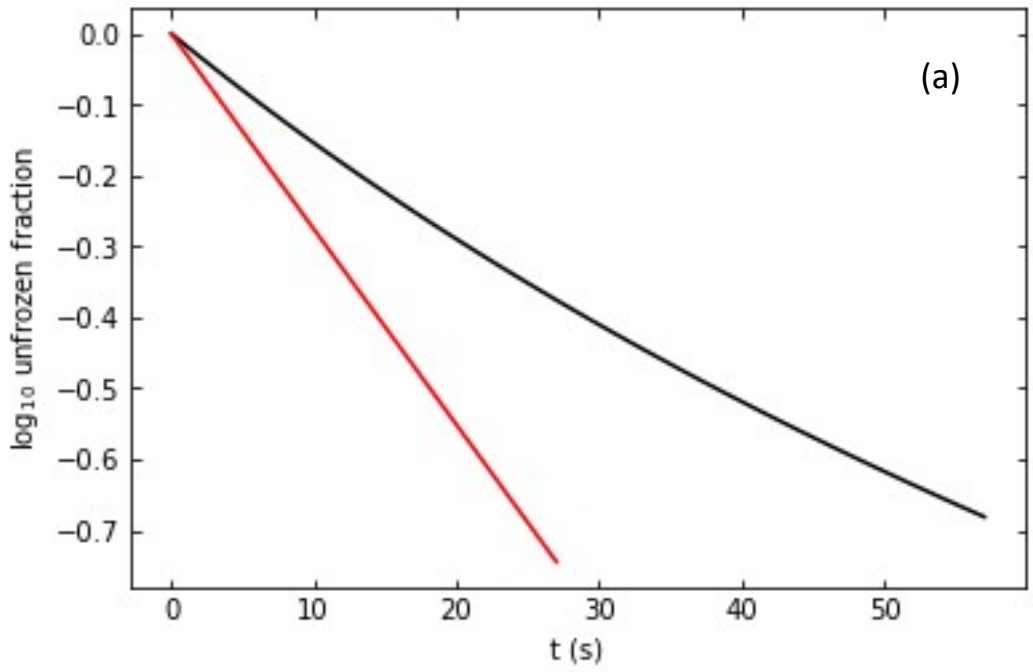

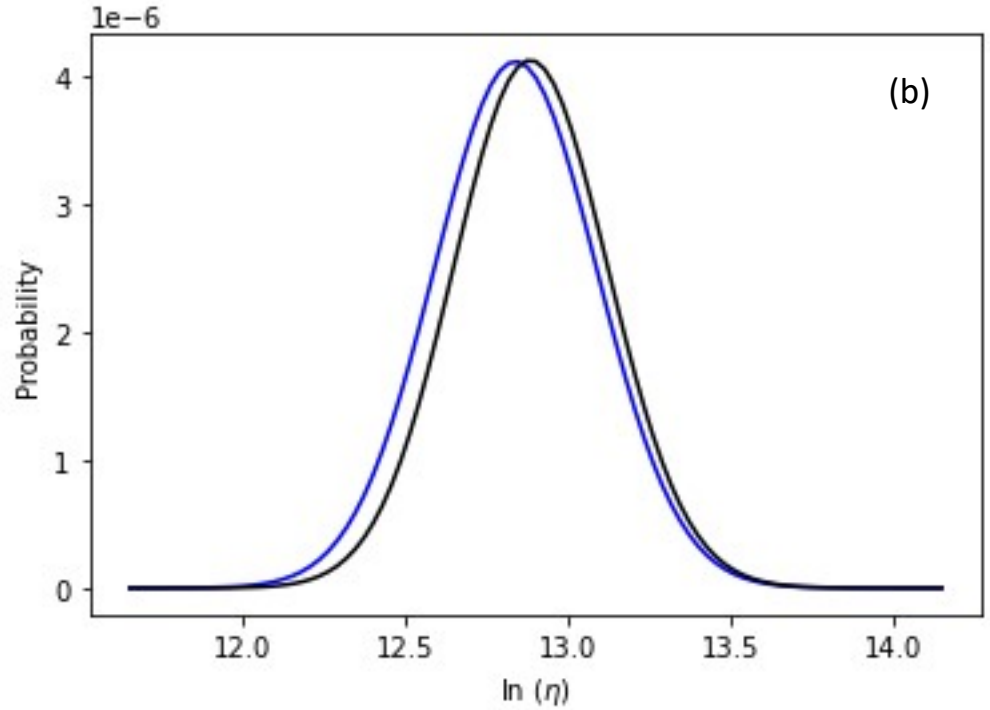

Figure S4. (a) As figure S3, except that the effect of a ramp from 0 °C to -24.5 °C at 50 °C /min and holding the temperature at -24.5 °C for $2\ s$ on the probablility distribution $P(\eta)$ was incorporated. (b) $P(\eta)$ before (blue line) and after (black line) the ramp and hold. The fraction of droplets that was predicted to freeze during the ramp and hold was 20% for the annealed origami and 22% for the unannealed.

Log normal fits applied to data for unannealed DNA samples

To fit the $U(t)$ (unfrozen fraction) data for the unannealed DNA samples that are plotted in figure 2 and figure S2 (isothermal freezing) we assume a log normal distribution of η (see main text), $P(\eta)$, for the rare INAs responsible for their freezing.

This leads to

$$U(t) = \int P(\eta)\exp\{-R(T,\eta)\,t\}\,d\eta \qquad [S.1]$$

where

$$P(\eta) = \frac{1}{\eta\sqrt{2\pi}\sigma_\eta}\exp\,-\frac{(\ln\eta' - \mu_\eta)^2}{2{\sigma_\eta}^2}. \qquad [S.2]$$

and

$$R(T,\eta) = J_0\exp\,-\frac{\eta}{T(T-T_m)^2} \qquad [S.3]$$

Here η' is the dimensionless quantity $\eta' = \frac{\eta}{K^3}$. We can use P(η) and $R(T,\eta)$ as defined by equations [S.2] and [S.3] to model the frozen fraction $F(T)$ in a temperature ramp experiment. We integrate the equation [S.4]

$$dF(T,\eta) = (1 - F(T,\eta))\,R(T,\eta)\frac{1}{\alpha}\,dT$$

numerically to obtain $F(T,\eta)$, the frozen fraction as a function of η. Then $F(T,\eta)$ is weighted by the probability of the corresponding η to give

$$F(T) = \int P(\eta)F(T,\eta)d\eta \qquad [S.5]$$

Temperature (°C)	J_0 (per second, per droplet)	μ_η	σ_η
-24	0.54±0.06	12.7±0.1	2.7±0.4
-24.5	0.55±0.06	12.5±0.2	3.6±0.6
-25	0.5±0.1	11.7±0.5	2.3±0.8
-25.5	0.5±0.3	11.9±0.8	1.5±0.9
-26	0.39±0.04	9.8±1.4	4.7±1.9
-26.5	1.3±1.2	12.6±0.7	1.2±0.6

Table S1: Values of J_0, μ_η and σ_η used to model the unfrozen fraction data of figures 2 and S2 at the given temperatures. The corresponding median value of the fitted log-normal distribution of η is equal to $\exp(\mu_\eta)\ K^3$

Sample sizes

Temperature	-24°C	-24.5°C	-25°C	-25.5°C	-26°C	-26.5°C
Total number of unfrozen droplets at $t = 0\ s$	89	74	63	50	37	31
Number of combined runs	7	7	6	6	4	4
Estimated frozen fraction at $t = 0\ s$	36%	47%	48%	58%	54%	61%

Table S2: Sample sizes for isothermal measurements of unannealed origami.

Temperature	-24°C	-24.5°C	-25°C	-25.5°C	-26°C	-26.5°C
Total number of unfrozen droplets at $t = 0\ s$	143	127	98	70	74	60
Number of combined runs	10	10	9	7	8	8
Estimated frozen fraction at $t = 0\ s$	29%	37%	46%	50%	54%	63%

Table S3: Sample sizes for isothermal measurements of annealed origami tiles.

	Annealed (well-folded) Origami	Unannealed Origami	Buffer
Total number of droplets	50	52	49
Number of experimental runs	4	4	4

combined to give this total			

Table S4: Sample sizes for the data of Figure 4

Droplets that freeze before the start of an isothermal experiment

In addition to data for the precise number of unfrozen droplets included in each isothermal investigation, tables S2 and S3 present the estimated frozen fractions at $t = 0$, calculated assuming 20 droplets per run. Note that these frozen fractions increase with decreasing temperature as expected. The reason that the unfrozen fractions in tables S2 and S3 are still significant at temperatures for which the frozen fraction in figure 4 reaches values close to 1.0 is that the cooling rate prior to starting an isothermal experiment (50 °C /min) is much greater than for the temperature ramp experiment of figure 4 (1 °C /min). See figure S5.

Note also that the annealed origami sample frozen fraction, while lower than the unannealed origami frozen fraction at $T = -24.0℃$ is higher than the unannealed origami frozen fraction at $T = -26.5℃$. An increase in the annealed origami frozen fraction relative to the unannealed frozen fraction as the temperature decreases is exactly what is predicted by the model used to fit the data of figure 4 (see figure S5). This shows that data from isothermal and temperature ramp experiments are consistent with the same theory and therefore with each other.

Since droplets containing the most efficient INAs will freeze first, we expect that for unannealed DNA samples, the effect of droplets freezing prior to $t = 0$ will be to reduce the freezing rate and therefore the gradient of the experimental log $U(t)$ at any given value of t. Figure S4 (a) shows that our simple model captures this effect. A comparison of figure S4 (a) with figure S3 shows that the effect of incorporating the initial cooling ramp and a hold of $2\ s$ at $T = -24.5℃$ in the simulation is simply to make the log $U(t)$ curve slightly more shallow. Figure S4 (b) shows how the cooling ramp and hold influence the calculated distribution of $P(\eta)$.

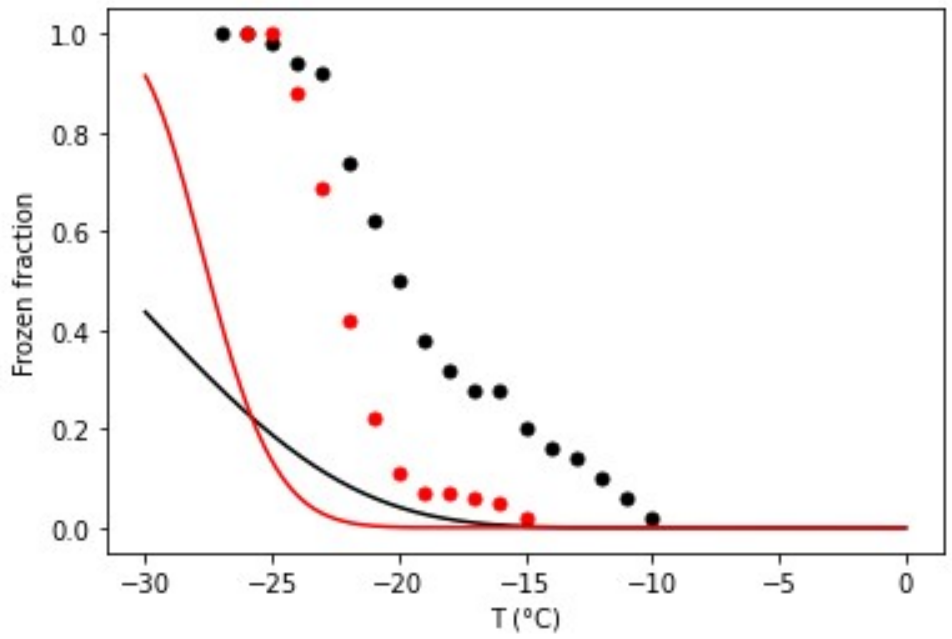

Figure S5. As figure 4 (main text) except that the modelled cooling rate was 50 °C /min rather than 1 °C /min.

Classical nucleation theory – derivation of equation [3] from main text

According to classical nucleation theory (CNT), the rate J at which new nuclei form can be written as

$$J = J_0 \exp\left(-\frac{\Delta G^*}{k_B T}\right),$$

where J_0 is a pre-factor, ΔG^* is the free energy barrier to nucleation, k_B is Boltzmann's constant and T is the temperature [3]. In the absence of a heterogeneous ice nucleating agent (HNA), ΔG^* is given by equation [3] of the main text:

$$\Delta G^* = \frac{16\pi\gamma^3}{3\Delta\mu^2},$$

where γ is the free energy per unit area of the ice-water interface and $\Delta\mu$ is the excess free energy of liquid water compared to solid ice per unit volume of the latter [3]:

$$\Delta\mu = \Delta H - T\Delta S.$$

Here $\Delta H = H_{liq} - H_{ice}$ and $\Delta S = S_{liq} - S_{ice}$. At T_m, the equilibrium melting point of ice, $\Delta\mu = 0$, so

$$\Delta S = \frac{\Delta H}{T_m}.$$

Hence (neglecting the dependence of ΔH or ΔS on T)

$$\Delta\mu = \Delta H\left(1 - \frac{T}{T_m}\right).$$

Since in this approximation ΔH is equal to L, the latent heat of fusion of ice (per unit volume) we can substitute for $\Delta\mu$ to obtain [4,5]

$$\Delta G^* = \frac{16\pi\gamma^3 {T_m}^2}{3L^2(T - T_m)^2}$$

In the presence of a HNA that reduces ΔG^* by a factor f, we can write

$$J = J_0 \exp\left(-\frac{16\pi\gamma^3 {T_m}^2 f}{3k_B L^2 T(T - T_m)^2}\right).$$

This is equation [3] of the main text.

References for Supporting Information

1 Jocher, G. *et al.* ultralytics/yolov5: v7.0 - YOLOv5 SOTA Realtime Instance Segmentation. (2022). https://doi.org/10.5281/zenodo.7347926

2 Dunn, K. E. *et al.* Guiding the folding pathway of DNA origami. *Nature* **525**, 82-86 (2015). https://doi.org/10.1038/nature14860

3 Sosso, G. C. *et al.* Crystal Nucleation in Liquids: Open Questions and Future Challenges in Molecular Dynamics Simulations. *Chem. Rev.* **116**, 7078-7116 (2016). https://doi.org/10.1021/acs.chemrev.5b00744

4 Turnbull, D. Isothermal Rate of Solidification of Small Droplets of Mercury and Tin. *The Journal of Chemical Physics* **18**, 768-769 (1950). https://doi.org/10.1063/1.1747765

5 Toner, M., Cravalho, E. G. & Karel, M. Thermodynamics and kinetics of intracellular ice formation during freezing of biological cells. *J. Appl. Phys.* **67**, 1582-1593 (1990). https://doi.org/10.1063/1.345670